LA-UR- 00-2985

Approved for public release; distribution is unlimited.

Title: HIGH ENERGY X-RAY AND NEUTRON MODELING AND DIGITAL IMAGING FOR NONDESTRUCTIVE TESTING APPLICATIONS

Author(s): Anthony W. Davis
Charles R. Hills
Matthew J. Sheats
Thomas N. Claytor

Submitted to: SPIE Annual Meeting, August 2, 2000

Los Alamos
NATIONAL LABORATORY

DISCLAIMER

HIGH ENERGY X-RAY AND NEUTRON MODELING AND DIGITAL IMAGING FOR NONDESTRUCTIVE TESTING APPLICATIONS

Anthony W. Davis*, Charles R. Hills, Matthew J. Sheats, Thomas N. Claytor
ESA-MT, Los Alamos National Laboratory, MS C914, Los Alamos, NM 87545

ABSTRACT

Adapting amorphous silicon imagers to the rigors of nondestructive evaluation has required the creation of new tools and techniques for successful detection of flaws in dense objects. At Los Alamos National Laboratory, extensive use of digital imagers and a desire to replace film with digital systems has led to additional research into modeling and simulation with an ultimate goal of improved techniques for using these imagers. The imagers have been used with varying success at x-ray energies ranging from 70 keV to 20 MeV, as well as with a variety of neutron energies at the Los Alamos Neutron Science Center (LANSCE). To simulate these diverse situations, a new version of the Monte Carlo Neutron/Photon (MCNP) simulation package, developed at Los Alamos, is employed (MCNP-X). The rapid simulation of various setups allows the rapid development of techniques without extensive and costly experimentation or test blocks. The simulations cover digital radiography as well as computed tomography. The results of these simulations leads to several techniques for digital radiography and computed tomography unique to amorphous silicon imagers, and provides additional information concerning the transition from film to digital imaging. Specifically, techniques have been developed to use the order of magnitude speed advantage of amorphous silicon detectors to provide density resolution in ways not possible with film. Also, the viability of amorphous silicon detectors at extremely high energies (1-20 MeV) is simulated and tested experimentally.

Keywords: Monte Carlo Simulation, MCNP, amorphous silicon, high-energy radiography, radiography, simulated radiography, neutron radiography, computed tomography simulation.

INTRODUCTION

Radiography has long been established as a reliable and robust method of nondestructively evaluating many parts of industrial interest. Welds, material properties, and conformance to design can be readily examined through this established process. The procedure for radiography has remained essentially unchanged for decades: an x-ray source illuminates the object of interest and the attenuated beam is measured using photographic film. Once the film is developed, the image is analyzed and measurements are made using a lightbox or microscope. Electronic detectors have been available for many years, but their low resolution and high noise limited their use to a very few applications. They were not well suited to the rigorous specifications of industrial nondestructive analysis. In the past few years, a new generation of detectors have emerged yielding performance comparable to film, and finally it has become reasonable to propose their use as a replacement to film detection.

The transition to digital detectors requires a thorough investigation of the technical performance of the detectors compared with film as well as proposing correct use of digital detectors. Many questions arise as soon as a different detection system is proposed. There are obvious questions of spatial and contrast resolution and noise, but other non-obvious issues remain regarding physical installation, energy issues, image interpretation, archiving, training, and analysis repeatability. In short, replacing film with digital detectors does not involve simply removing film cassettes and replacing them with digital panels. There are still some applications for which digital detectors cannot replace film, and it is important to identify exactly the parameters for which digital detectors are superior or inferior to film. Ultimately, for most applications, a digital detector based radiography system is functionally equivalent to a film system.

The digital detection system that currently performs most acceptably as a replacement for film is based on large format amorphous silicon detector plates. These detectors are available from a variety of vendors, but their performance and specifications are very similar. The nominal amorphous silicon detector is 10 by 16 inches in area with around 130 micron pixel to pixel spacing. These detectors have the best resolution available in a package that will endure the high radiation of industrial radiography and provide immediate (less than one minute) images.

* Email: awdavis@lanl.gov

In order for this technology be successfully implemented, there must be parallel developments in theory and practical approach. These efforts can be greatly accelerated by making use of simulation tools that other disciplines have been using for decades. NDE simulations are useful for understanding phenomena, conceiving and qualifying methods and demonstrating their performance at low cost, teaching and training operators, and providing additional guidance to experts in the field. Simulation tools are an essential part of models-based inversion algorithms that allow automated feature recognition. Optimization of inspection protocols & procedures will significantly improve confidence in radiographic and CT inspections, something which is now currently heavily reliant on operator experience.

1. DIGITAL RADIOGRAPHY CHARACTARISTICS

The first step in moving from film imaging to digital imaging is to know the parameters of data acquisition and optimize the acquisition process for the detector. This includes knowing the capabilities of the digital detectors and determining if a setup can measure the features of interest to within the required specifications. Therefore, the characteristics, resolution, and techniques for use of amorphous silicon or other area digital detectors must be well known and compared with film.

1.1. Characteristics of Digital Detectors

Area digital detectors, including amorphous silicon based detectors, are available from a variety of manufacturers, and their specifications are rapidly improving. At their most basic level, they all consist of an imaging area composed of an array of individual point detectors, or pixels. Each detector can differentiate between some finite number of levels defining the intensity of the x-ray at that point. Since the detector has finite and discrete measurements, it can be said that the detector digitally samples both in space and intensity. The resolution of the spatial sampling is determined by the spacing between the pixels and the scintillator, and is measured in linepairs per millimeter. The intensity sampling is determined by the analog to digital conversion performed on the individual pixels, measured in bit depth (typical detectors use 12 bit A/D converters, resulting in 2^{12} discrete intensity levels, or 4096 levels). Typical detectors have a dynamic range of around 2000:1. They are constructed by placing a large amorphous silicon detector etched to produce the millions of individual light detectors that can be pressed directly against a scintillating screen. This produces an extremely efficient x-ray detector, since all the light output by the scintillator is incident on the photodiodes (i.e., there are no lossy optics.)

The amorphous silicon detector area is inherently insensitive to radiation damage, so it is well suited for the rigors of use in industrial x-ray bays. The supporting electronics surrounding this detection region, however, are not insensitive to radiation damage. It is therefore important to shield the support electronics from the primary x-ray source. If precautions are taken, the detector should withstand normal use for several years, even in extremely high radiation areas. The mode of failure due to radiation damage ranges from dramatically degraded images to complete failure of the detector.

1.2. Spatial Resolution Comparison

Spatial resolution is the most obvious criteria for comparison between film and digital detectors. It is also the area in which film has the most pronounced advantage. In short, current amorphous silicon detectors can resolve about 4 linepairs per millimeter, where standard M film can easily resolve 20 linepairs per millimeter. Film is limited only by grain size, and the randomly arranged grains are nominally 20 microns in diameter. This allows film to achieve extremely high resolutions. Two features limit digital area detectors: the scintillator and the pixel spacing. In order to fully understand detector resolution, the relationship between the scintillator and the geometry of the detectors must be explored. In addition, the idea of geometric magnification of a part to achieve better resolution has particular limitations and advantages with digital detectors. There are, in fact, several interesting facts about digital area detector resolution.

A digital area detector is at its core a digitally sampled system, and therefore it conforms to standard signal theory for sampled systems. Nyquist sampling would therefore require that the maximum spatial frequency (in linepairs/millimeter) would be determined by

$$f_N = \frac{1}{2\Delta d}, \qquad \text{Equation 1}$$

where f_N is the Nyquist limited frequency (half the sampling frequency) and Δd is the detector-to-detector spacing. This is not the entire story, as the imaging array is two-dimensional and the pixels are square. Therefore, the maximum frequency has a direction component, θ, as well:

$$f_N = \frac{1}{\Delta d\sqrt{2}\sin(2\theta) - 2\Delta d\sin(2\theta) + 2\Delta d}. \qquad \text{Equation 2}$$

This result can be seen practically in Figure 1, a set of radiographs of a linepair gauge taken with the dpiX Flashscan 20 digital imager. The Flashscan 20 has a detector to detector spacing of 0.127 millimeters, yielding about 4 linepairs per millimeter at 0 degrees and 5.5 linepairs per millimeter at 45 degrees.

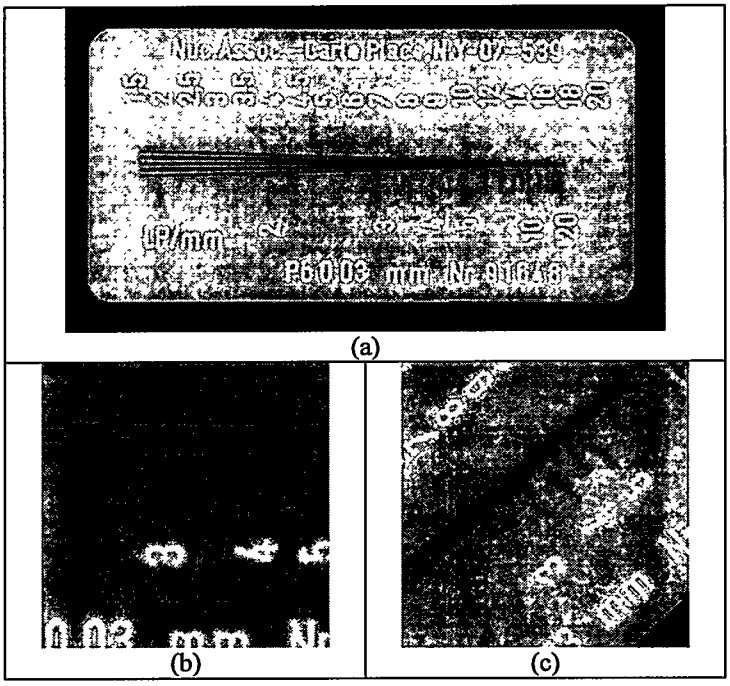

Figure 1. Linepair gauges illustrating resolution at the detector plane for different angles. Image (a) is a radiograph of the overall linepair gauge on a dpiX Flashscan 20 (127 micron pixel spacing). Image (b) is a close-up of the gauge at 0 degrees showing about 4 linepairs per millimeter. Image (c) is a close-up at 45 degrees showing about 5.5 linepairs per millimeter.

An important feature of the calculated sampling frequency is that it not only represents the maximum frequency the detector can sample, but it also represents the maximum frequency of images incident upon the detector allowed before aliasing. In other words, a system should be set up in such a way that the incident x-ray pattern *does not exceed* the sampling frequency of the detector. Clearly, if the incident x-ray pattern has lower frequency content than the detector, the image will be fully sampled. However, if the incident x-ray pattern has higher frequency content than the detector, it will be aliased. This phenomenon is well known in other types of digital sampling: sampled signals must be band limited to half the sampling frequency. The somewhat counterintuitive result is that the image must be blurred slightly in order to reduce image degradation. A better way of putting it is that the incident image must be optimally matched to the detector. Aliasing can be seen as undesirable patterns emerging in areas of high frequency content (Figure 2).

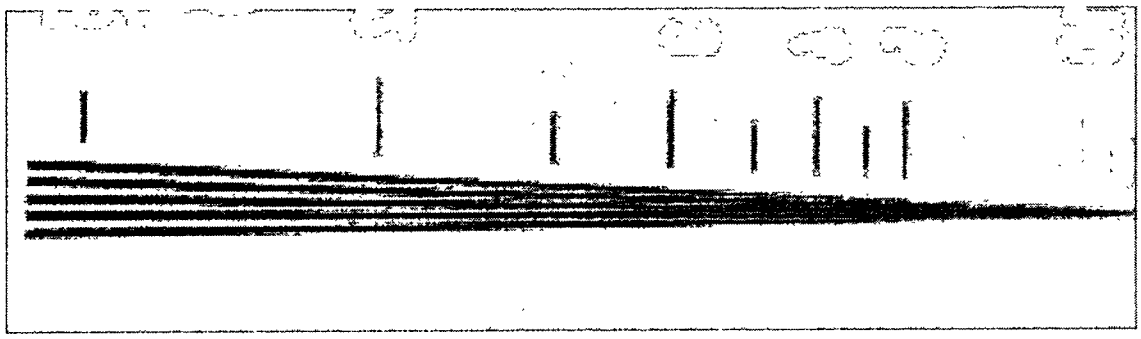

Figure 2. Spatial aliasing is evident in this linepair gauge near four linepairs per millimeter. The pattern in the high frequency lines is due to aliasing.

In digital imagers, there are two ways to band limit the incident signal. The first method is to match the scintillator to the detector array. Scintillators have inherent spatial frequency responses, and a scintillator that limits response to the sampling frequency of the detector will prevent aliasing (in normal A/D conversion, this is referred to as a bandwidth-limiting filter.) Unfortunately, the frequency response of scintillators tends to fall off over a large frequency range, resulting in both loss of definition and aliasing in the same image (decreasing the signal to noise ratio). The ideal prefiltering scintillator would have full response to frequencies below the sampling frequency, and then fall to zero response to frequencies above the sampling frequency. In reality, most scintillators have lower than full response below the sampling frequency and much higher than desirable response above the sampling frequency. Figure 3 shows the frequency response for several Kodak Lanex scintillators. A frequently used scintillator is Lanex Fine, which has good frequency response below the sampling frequency (4 linepairs per millimeter) but continues to respond above the sampling frequency (not shown on this graph).

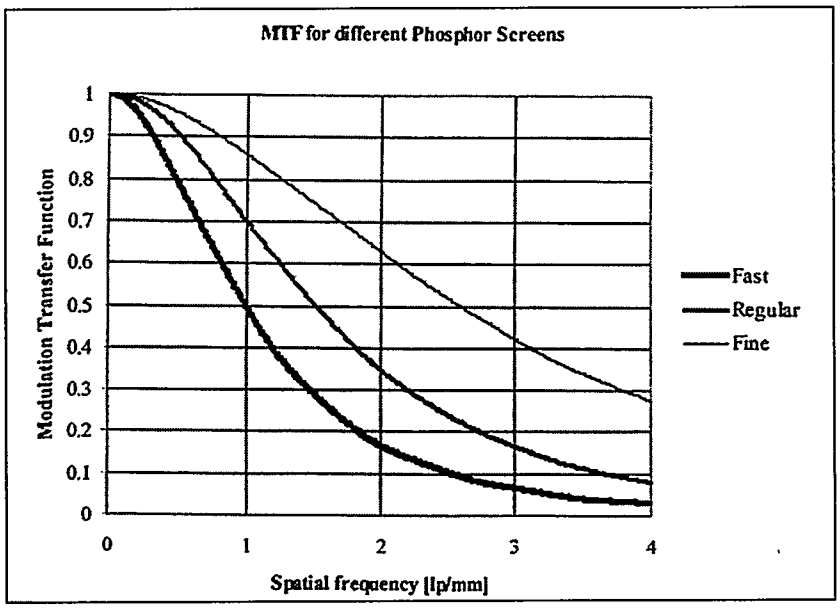

Figure 3. DpiX published MTF for the Flashscan 20.[1]

The second method of band-limiting the incident x-ray pattern is to adjust the geometry of the source-object-detector system to use the finite source spot size to blur the image to match the detector. This is the preferred method of band-limiting images, as it provides the best signal to noise ratio and resolution. It also ensures the best possible resolution of the object being inspected. Ultimately, the detectible resolution in any part is limited primarily by the pixel-to-pixel spacing of the detector and the spot size. These two parameters alone will determine the required magnification to achieve maximum resolution without aliasing and the minimum resolvable feature.

The bottom line is the resolvable feature size depends mostly on the source spot size. Tradeoffs exist between different parameters such as spot size and x-ray flux, but ultimately the speed of digital detectors (4000 times faster than M film in terms of image exposure time alone) make many of these tradeoffs much more palatable. Table 1 shows that for microfocus x-ray machines, digital detectors can perform nearly as well as film in terms of detectable features. For larger spot size machines, the lower resolution of the digital detector limits the resolvable features, and the difference between film and digital imaging is more noticeable. Figure 4 shows the energy applications and resolutions possible with digital imaging and film.

Another pair of parameters for tradeoff in achieving these resolutions with flat panel area detectors is source flux and overall viewable area. As the magnification increases and the panel moves further from the source, there is significantly less flux available at the detector, but more importantly, the available imaging area decreases dramatically. At the maximum magnification indicated on Table 1 of 64 times, even a small part will fill the entire detector.

Table 1. Resolvable feature size comparison between film and digital.

Source spot size	Film detectable feature size	DpiX Flashscan 30 detectable feature size
0.002 mm	0.0036 mm	0.0039 mm
0.01 mm	0.013 mm	0.018 mm
0.400 mm	0.038 mm	0.193 mm
1 mm	0.039 mm	0.225 mm
2 mm	0.040 mm	0.239 mm
4 mm	0.040 mm	0.246 mm

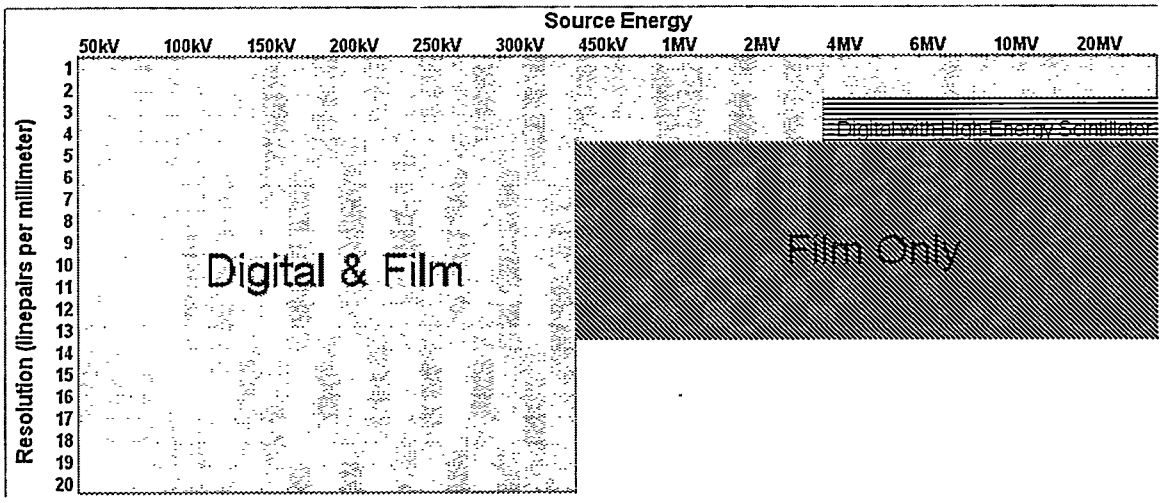

Figure 4. Chart showing the practical range of digital imaging given general spot sizes and behavior of sources at different energies. The left area indicates where both digital and film are acceptable. Red indicates areas where only film will currently perform well. Film is still preferred for high-energy, high-resolution applications. However, for the majority of applications, including some high-energy applications, digital imaging performs as well or better than film. Some high-energy applications are possible with digital detectors only with special scintillators[2], as is indicated in the small area to the top right.

1.3. Dynamic Range Comparison

An important measure of radiographic detection is how well the system (employing either a film or digital detector) can resolve small variations in intensity. This property is called dynamic range or contrast resolution. It is a measure of the entire radiographic system, not just the detector. Film and digital detectors have such dissimilar responses that this comparison is very difficult. Ultimately, film and digital detectors have very similar overall dynamic ranges, but for completely different reasons.

Film has two key features that give it its wide dynamic range. First, it has very low noise. The chemical process film uses is not prone to be noisy. Each grain responds very similarly to every other grain. It can be exposed over extremely long periods of time without degrading the image significantly. Its second feature is its graceful saturation. When sections of the image are overexposed, no other areas of the image are affected. Therefore, it is acceptable to overexpose the outside of a part without affecting the interior image. It is generally accepted that film can resolve density differences of around 1% with proper setup. The price for these desirable features is extremely slow exposure times.

Digital detectors have several features that allow them to achieve similar performance. Their moderate noise can be compensated by taking multiple images and averaging (the electronic noise is zero mean and can be reduced by averaging). Also, their extremely fast exposure times allow lower energies to be used, accentuating the contrast for a particular object. Using these techniques, digital imagers can actually produce images with greater contrast resolution than film. As an example, a phantom was created to test both spatial and density resolution (Figure 5). The phantom was imaged at 110 kV with the digital detector for 40 seconds. The same exposure with film would have required almost 44 hours of exposure. Of course, with its lower noise floor, film can use higher energies and still resolve the same image in a few minutes.

Unlike film, many digital detectors cannot produce acceptable images if portions of the detector are overexposed. This has important consequences for radiographic setup, as often portions of images are intentionally overexposed to correctly expose other portions. This is especially true with curved parts. Care must be taken with digital detectors to mask portions of the image that would normally be overexposed to prevent general image degradation.

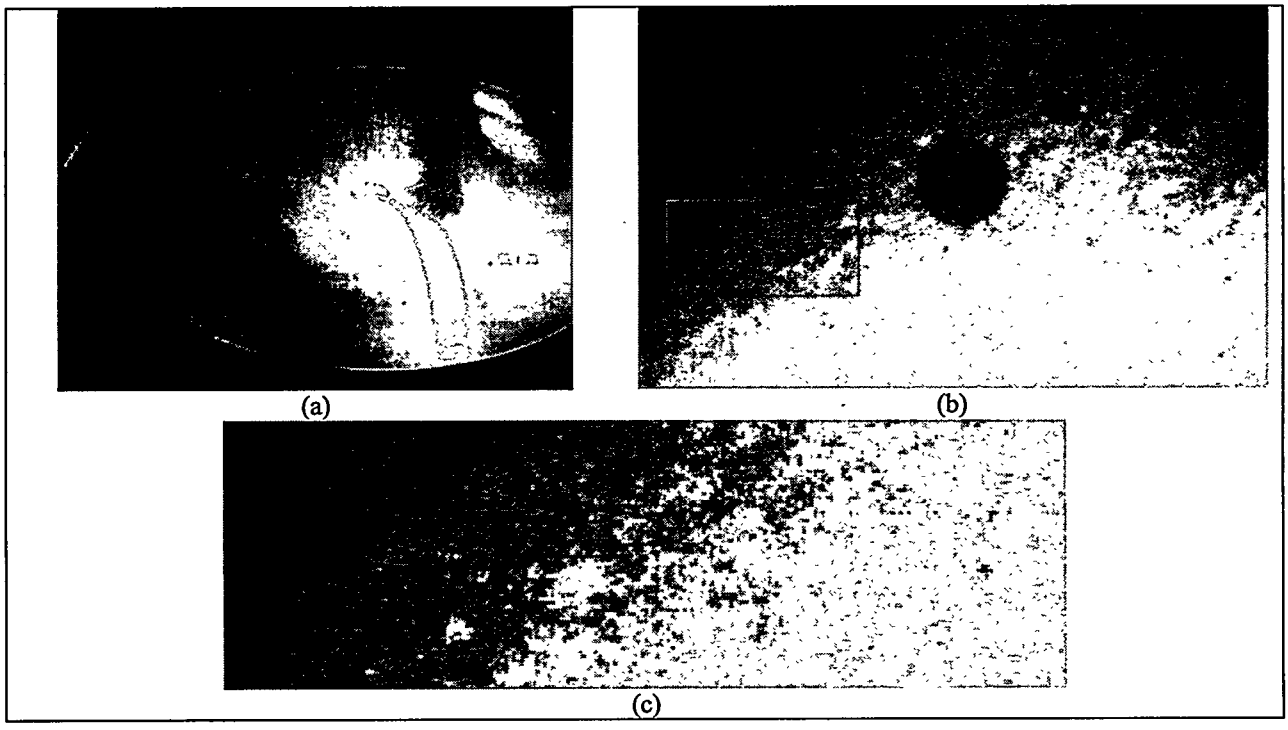

Figure 5. Phantom illustrating 1% density differences. Image (a) shows a photograph of the 8-inch diameter copper phantom. Images (b) and (c) show the digital radiograph of the phantom at different magnifications. The mottled appearance is a result of density variations within the copper. The smallest feature is 300 microns in diameter and 100 microns deep in 10-millimeter thick copper. The feature is easily identified with digital radiography, but not as easily found with film.

RADIOGRAPHIC SIMULATION

In this report, we concern ourselves with computer simulation of radiation transport as applied to non-destructive evaluation (NDE) using the high energy version of the Monte Carlo code MCNP[3] called MCNPX[4]. Lawrence Livermore National Laboratories published a very nice report documenting some results of radiograph simulations with the COG radiation transport code. It is thus conceivable that simulations for NDE will be a normal mode of operation similar to the use of design tools for other disciplines in engineering and science. Advancements in computer hardware in addition to the Monte

Carlo variance reduction improvements that have been, and continue to be made with the MCNPX source code, have brought many of the "advanced" applications of this code to a much brooder user group than previously available. In this report, we discuss the application of MCNPX to radiographic non-destructive evaluation (NDE).

1.4. Motivation for Simulation

With no new designs of nuclear weapons and the unexpected extension of the lifetime of US nuclear weapons, non-destructive inspection and testing now plays an even more important role in demonstrating the integrity, health, and safety of the nuclear weapons stockpile. In particular, radiographic techniques (CT, digital radiography, neutron radiography etc.) are being looked at to help with this challenging life extension of the stockpile. It important that if we are to extend the lifetime of these weapons further than their design intent, that we continually strive to make advancements in this technology. In order for this technology of NDE to advance like this, there must be parallel scientific developments in knowledge and understanding. These increases can be greatly accelerated by making use of simulation tools that other disciplines have been using for decades. NDE simulations are useful for understanding phenomena, conceiving and qualifying methods and demonstrating their performance at low cost, teaching and training operators, and providing additional guidance to experts in the field. Simulation tools are an essential part of models-based inversion algorithms that allow automated feature recognition. Successful integration of simulation into our NDE program will constitute a giant step toward achieving the Laboratory' stated goal of a zero-defect science-based stockpile stewardship program.. Optimization of inspection protocols & procedures will significantly improve confidence in radiographic and CT inspections, something, which is now currently heavily reliant on operator experience. We will be able to rationally defend our answers to questions such as "How do we know we have the best inspection possible?" "Can we be sure that a flaw of a certain size and/or composition will be seen?" "How many views and what pixel density are required in to ensure resolution of critical defects of a certain type and size in a CT inspection?" "How can we be sure new CT reconstruction algorithms are valid?" and "Once we have optimum exposure parameters for what we think we have (the as-built part), what can we expect upon inspection or re-inspection if certain material parameters or inspection system configurations change?". These are important questions the answers to which we should have more than a passing understanding.

1.5. Los Alamos and the Monte Carlo Method

The Monte Carlo method dates back to the late eighteenth century. However because it is a statistical method that depends on very large sampling of random numbers, which makes it labor intensive, it was seldom used. The method, as applied to radiation transport, was first introduced by Stanislaw Ulam and further developed by John von Neumann shortly after Word War II. Its computational power was quickly recognized and it became an essential tool to help understand the complex phenomena in the design of the first hydrogen bomb. From that point on, Los Alamos has been working on development of Monte Carlo methods for radiation transport that have had a rich resume of applications.

The Los Alamos work on Monte Carlo methods has resulted in the MCNP (Monte Carlo N-Particle) code that can be used for neutron, photon, electron, or coupled neutron/photon/electron transport, including the capability to calculate multiplication constants for critical systems. Pointwise cross-section data are used. For neutrons, all reactions given in a particular cross-section evaluation are accounted for. Thermal neutrons are described by both the free gas model and the S(a,b) model. The S(a,b) thermal scattering treatment is a complete representation of thermal neutron scattering by molecules and crystalline solids. For photons, the code takes account of incoherent and coherent scattering, the possibility of fluorescent emission after photoelectric absorption, absorption in pair production with local emission of annihilation radiation, and bremsstrahlung. A continuous slowing down model is used for electron transport that includes positrons, k x-rays, and bremsstrahlung, but it does not include external or self-induced fields.

Important standard features that make MCNP very versatile and easy to use include a powerful general source, criticality source, and surface source; both geometry and output tally plotters; a rich collection of variance reduction techniques; a flexible tally structure; and an extensive collection of cross-section data.

The MCNP code has been widely used by the medical community for medical imaging applications[5]. As for industrial applications, the author knows of no use of MCNP of any significance. The Livermore radiation transport code COG has been applied for industrial applications[6].

1.6. The MCNPX Code

Recent advances in the radiation transport code MCNPX has provided ESA-MT a tool to be used for realistic simulations of CT and radiography scans. Historically, radiographic modeling and Computed Tomography at Los Alamos has been done with the Monte Carlo Code, MCNP (Unesaki, Hibiki, and Mishima, 1997, Hills, Brockhoff, and Estes, 1995; Geroge, et al, 1990). However, this code was not widely used for that type of modeling with the objective of generating a realistic image, it took a large amount of computer time for the direct images; the scatter could not be done at all in one lifetime. When an addition to the MCNP source code, the radiography patch, (the feature is a permanent inclusion in MCNPX, the high-energy transport version of MCNP) became available (Snow and Court, 1998), more realistic radiography/CT simulations were now feasible. The newly available radiography option now available in MCNPX allows one to generate direct images in very little time; with a little more time and effort the scattered image can also be generated. By incorporating the radiography patch in MCNP, or direct use of MCNPX, the user can easily set up a detector grid for any number of detectors and given resolution. Furthermore, the code has the ability to generate the direct or source contribution to the image, in addition to the total image obtained from both scattered and direct contributions. Also, a new mesh tally was developed that allows the user to subdivide space into many small volumes in an easy manner. In this way, one can score flux, energy deposition, etc. in these volumes and generate radiation patterns as a function of position in the geometry. Simulations with MCNPX can now be done to determine methods for image enhancement or to extract a direct image from one composed of direct, scattered, and background contributions.

1.7. Neutron Radiographic Simulation Results

As a first example we will demonstrate the radiographic capabilities of MCNP in modeling a low energy neutron radiography experiment that was performed at the Los Alamos Neutron Scattering Facility (LANSE). The model of the experiment is shown in Figure 6.

In three separate experiments, the block was exposed to monoenergetic thermal neutron beams as shows in the Sabrina simulation in Figure 7. The three energies used for the experiment were 0.0077eV, .0025eV, and 0.00152eV. These energies allowed us to demonstrate the effect that the cross sections for beryllium carbon influence the quality of the image of the various parts. It also serves as a good check to the simulation model to see if similar effects are observed. Figure 8 shows the target area of the experiments overlaid with the detector grid.

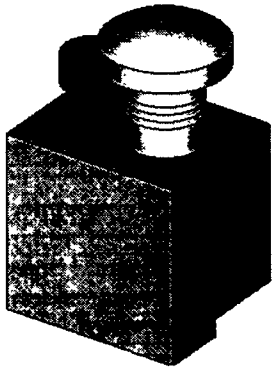

Figure 6. Cold Neutron Target consisting of a beryllium block (green) with a carbon (blue) and stainless steel bolt (red).

The results of the calculations are shown in Figure 4. It is apparent that the simulations predicted the qualitative results of the image very nicely. As shown in Figure 5, at 0.0077eV, the cross section for Be is larger than C and accordingly, the be block clearly obscures the carbon block. However, at 0.0025eV, the C cross section increases by an order of magnitude and the Be cross section stays about the same, thus more neutrons are penetrating the Be block and the carbon bolt is clearly resolved. The cross sections take another change at 0.0152eV and where the Be cross section is larger than graphite, and once again the carbon bolt is obscured in the Be block.

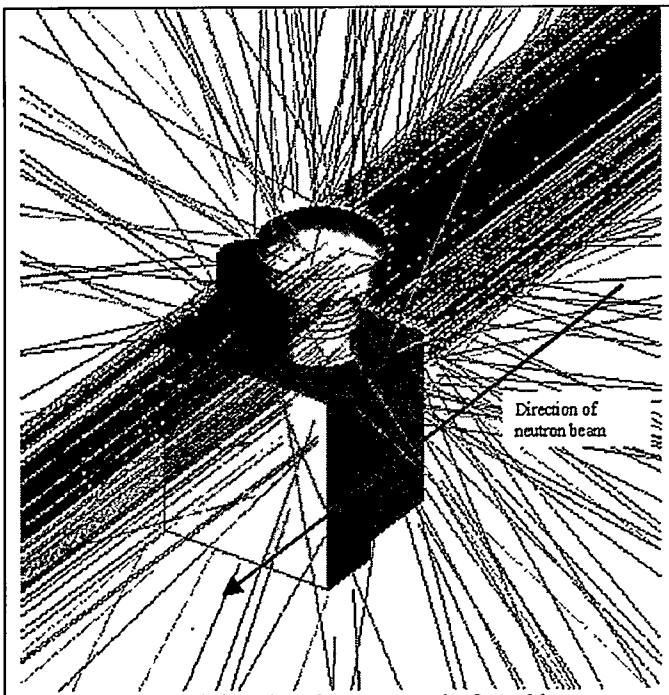

Figure 7. Sabrina plot of neutron tracks for cold neutron radiography simulation.

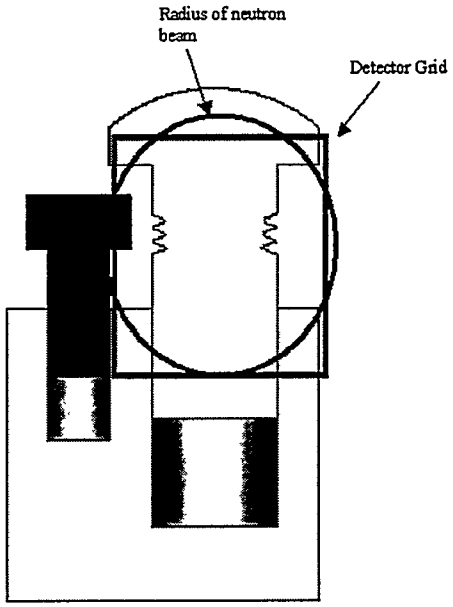

Figure 8. Approximate Cross section of the neutron target and detector area of the experiment and simulation.

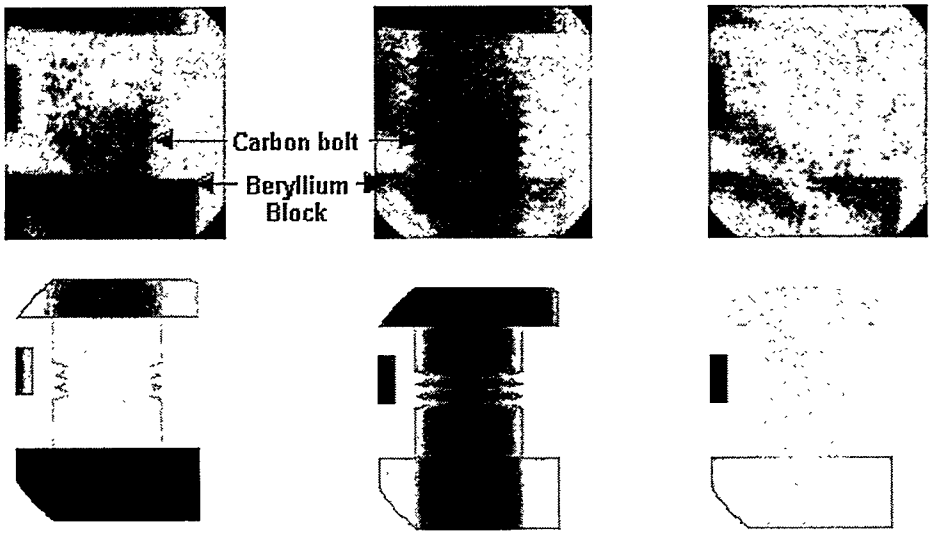

Figure 9. Results of the experiment (top) and simulation (bottom) for the thermal neutron radiography experiment. The simulated results qualitatively very well with the experimental results.

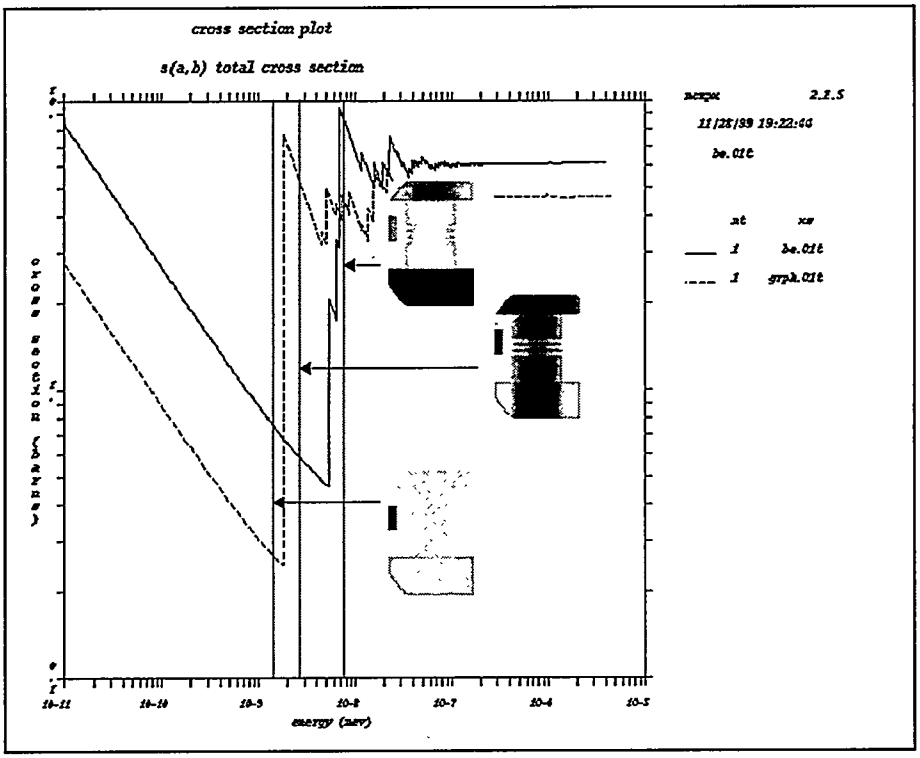

Figure 10. A plot of the cross sections for the various energies used for the experiments and the associated simulations showing clearly the effect of the neutron cross section on the resulting image as was observed in the experimental results.

1.8. Computed Tomography Simulation Results

In this section we present the results of a CT simulation and the comparison with experimental results. The model is shown in Figure 6. Several experiments were performed with this phantom with many different configurations. The use of simulation for computed tomography systems is a relatively recent innovation, and allows refinement of CT data acquisition and data handling techniques[7]. Only the simulation of the configuration presented in Figure 6 will be presented in this paper.

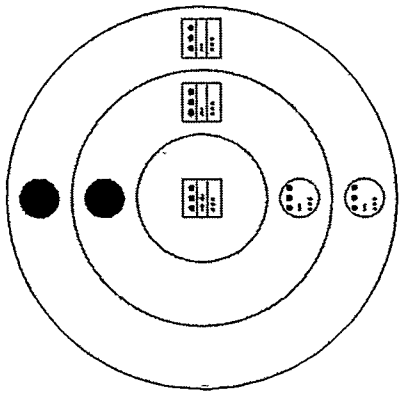

Figure 11. Cross section of the Allied Signal CT calibration blocks. The configuration modeled consisted of an aluminum cylinder and two rings and five aluminum inserts containing nine cylinders of three different sizes (0.5-mm, 1-mm, and 2-mm) filled with air and two large cylinders filled with water.

The x-ray source consisted of a 420kV tungsten tube filtered with 0.0625 inches of lead. Although the capability of modeling scattered radiation exists, for this simulation, only direct source contributions were used for this simulation. For the simulation as well as the actual data, 900 views were taken. The results are shown in Figure 7.

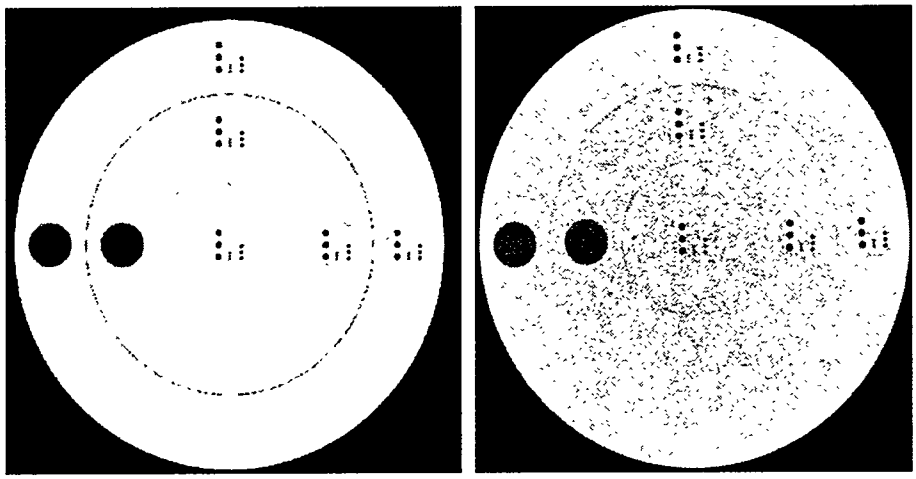

Figure 12 Comparison of simulated (left) with actual (right) CT scan of the Allied Signal Calibration Blocks. Only direct source contributions were scored for this calculation.

REFERENCES

1. R. L. Weisfield, M. A. Hartney, R. A. Street, and R. B. Apre, "New Amorphous-Silicon Image Sensor for X-Ray Diagnostic Medical Imaging Applications," SPIE Vol. 3336, Medical Imaging 1998, Physics of Medical Imaging, 22-24 February 1998, pp. 444-452.
2. A. W. Davis, C. R. Hills, M. J. Sheats, T. N. Claytor, "High Energy X-Ray and Neutron Modeling and Digital Imaging for Nondestructive Testing Applications," LA-UR-00-0104.
3. Briesmeister, J. F., MCNP4B Manual, LA-12625, March 1997.
4. Waters, L. S., MCNPXTM User's Manual, Version 2.1.5, TPO-E83-G-UG-X-00001, November 14, 1999.
5. Brockohoff, R.C, Estes,G, P., Hills, C. R., ,DeMarco J., C., and Solberg T, D., 1996 Application of MCNP to Computed Tomography in Medicine, LA-UR-96-135.
6. Buck, R. M., and Hall, J. M., Applications of the COG Multiparticle Monte Carlo Transport Code to Simulated Imaging of Complex Objects, Lawrence Livermore National Laboratory, UCRL-JC-134630, June 1999.
7. Hills, C. R., Brockhoff, R, C, and Estes, G. P, 1995, CT Scan Simulation with the MCNP Monte Carlo Code, Medical Physics, Vol. 22, No. 9, p. 1534